

1 Supplement of

2 **Cloud–Aerosol Classification Based on the U-Net** 3 **Model and Automatic Denoising CALIOP Data**

4
5 **Table S1.** Denoising Evaluation of 532nm Perpendicular Attenuated Backscatter

Denoising Techniques	SNR	RMSE	SSIM
Gaussian filtering	4.089	0.050	0.983
Three-point smoothing	2.419	0.061	0.974
Bilateral filtering	5.621	0.042	0.989
Median filtering	4.343	0.049	0.985

6
7 **Table S2.** Denoising Evaluation of 1064nm Attenuated Backscatter

Denoising Techniques	SNR	RMSE	SSIM
Gaussian filtering	2.918	0.018	0.995
Three-point smoothing	1.142	0.022	0.993
Bilateral filtering	3.799	0.016	0.996
Median filtering	3.307	0.017	0.996

8
9 Through the application of four denoising methods on 532nm Perpendicular Attenuated
10 Backscatter and 1064nm Attenuated Backscatter, SNR, RMSE, and SSIM evaluation results were
11 obtained, as shown in Table S1 and S2. The outcomes indicate that bilateral filtering exhibits
12 the best performance for both 532nm Perpendicular Attenuated Backscatter and 1064nm
13 Attenuated Backscatter, with evaluation results of 5.621, 0.042, 0.989, and 3.799, 0.016, 0.996,
14 respectively.

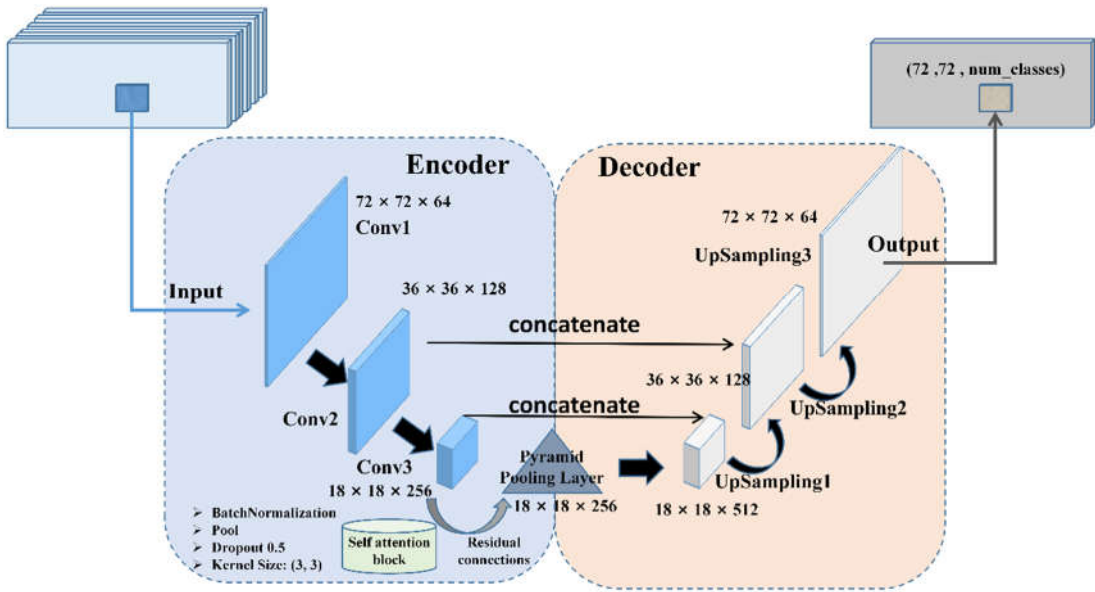
15
16 **Table S3.** Evaluating the Accuracy of Models Trained on Different Denoised Datasets

Denoising Techniques	Accuracy
Unreduced data	0.933
Gaussian filtering	0.948
Three-point smoothing	0.938
Bilateral filtering	0.953

Median filtering	0.945
------------------	-------

17
18
19
20
21
22
23
24
25

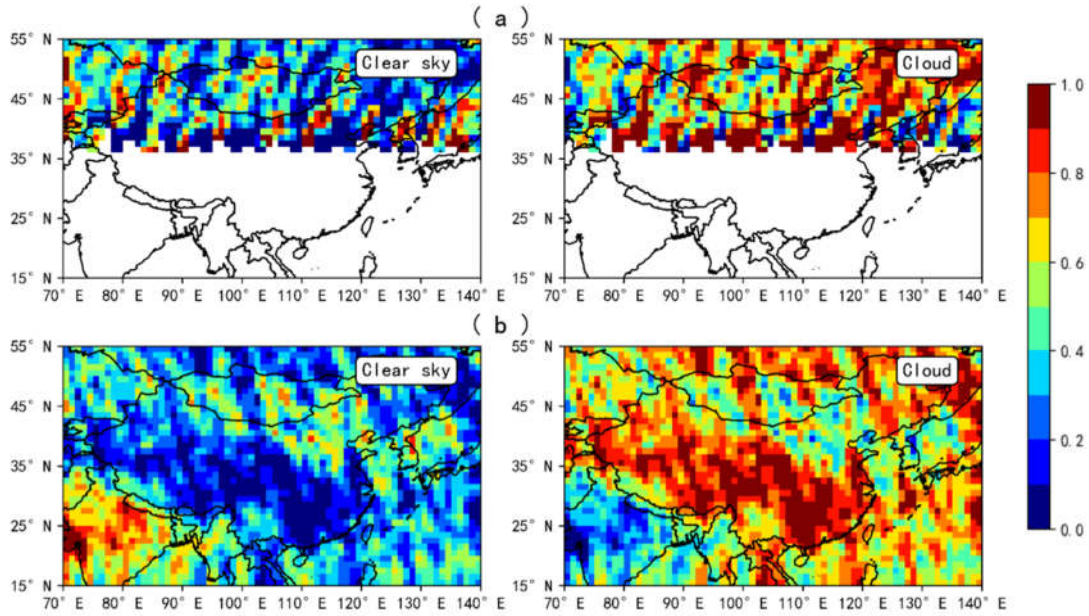
For a better comparison of different denoising methods, data processed by various denoising techniques were fed into the U-Net model. Table S3 presents the evaluation of model accuracy trained on different denoised datasets. It is evident that models constructed from denoised data exhibit higher accuracy compared to the non-denoised data. Among these methods, bilateral filtering demonstrates the best performance, achieving a U-Net model accuracy of 0.953.



26
27
28
29
30

Figure. S1 U-Net model structure.

The U-Net model construction diagram in Figure S1 is consistent with the main text's Figure 1. However, it features higher resolution and clearer details.



31

32 **Figure. S2** Cloud fraction maps generated by the CloudSat satellite's 2B-CLDCLASS-LIDAR product for the period from March 1 to May 31, 2019. (a) Nighttime; (b) Daytime. Significant missing values are present in the nighttime data.

34

35

36

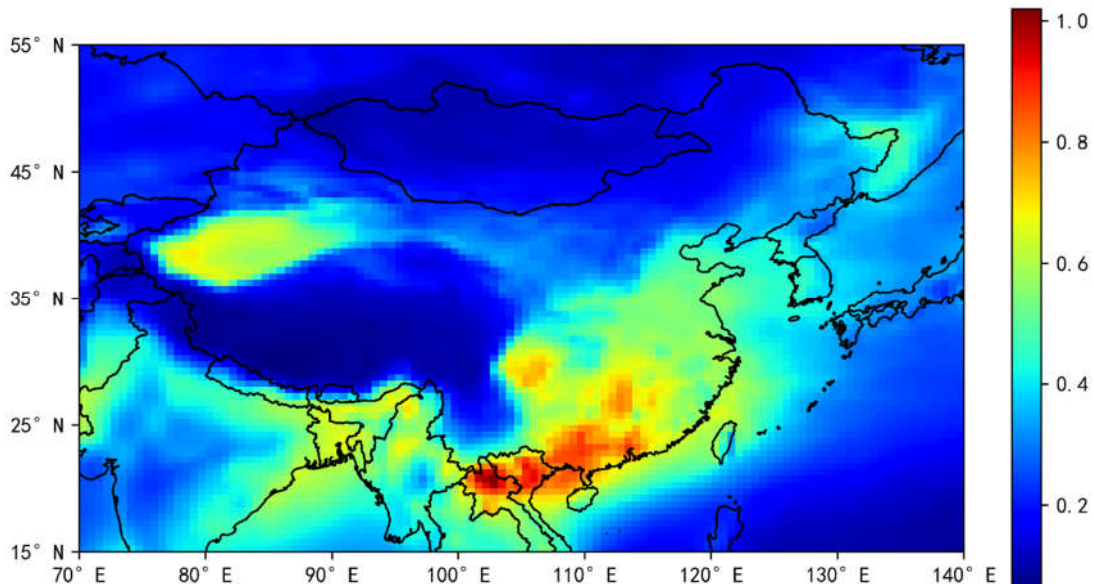
37

38

39

40

The study conducted a statistical analysis of the 2B-CLDCLASS-LIDAR product from the Cloudsat satellite for the period of March to May 2019, as illustrated in Figure S2. The aim was to compare it with the cloud identification results obtained from the U-Net model. However, it was observed that there is some missing nighttime data in the 2B-CLDCLASS-LIDAR product within this time range, while the daytime data remains intact.



41

42

43

44

45

Figure. S3 The monthly average Aerosol Optical Depth in MIRA2 during nighttime observations from March to May 2019.

Figure S3 displays The monthly average Aerosol Optical Depth in MIRA2 during

46 nighttime observations from March to May 2019, offering valuable reference information.